MEASUREMENT OF THE VELOCITY OF SOUND IN WATER BY OPTICAL METHODS

Thesis for the Degree of Ph. D.

MICHIGAN STATE UNIVERSITY
ARTHUR JARED CRANDALL

1967

THESIS

This is to certify that the

thesis entitled

MEASUREMENT OF THE VELOCITY OF SOUND
IN WATER BY OPTICAL METHODS

presented by

Arthur Jared Crandall

has been accepted towards fulfillment
of the requirements for

Doctor of Philosophy degree in Physics

E. A. Hiedemann
Major professor

Date 17 November 1967

O-169

MEASUREMENT OF THE VELOCITY OF SOUND IN WATER BY OPTICAL METHODS

by

Arthur Jared Crandall

AN ABSTRACT

Submitted to
Michigan State University
in partial fulfillment of the requirements
for the degree of
DOCTOR OF PHILOSOPHY
Department of Physics
1967

G 48447
3-7-68

ABSTRACT

Several new optical methods have been developed for the measurement of sound velocities in transparent fluids. The visibility pattern from stationary, progressive and pulsed progressive waves are detected by a fast response photomultiplier tube rather than visually, which allows the use of lower sound intensities. A theoretical expression is developed for the errors caused by diffraction in the near field of a circular transducer. The velocity of sound in distilled water was measured to be 1517.70 $\pm$ .20 m/sec. at a temperature of 34.00°C.

MEASUREMENT OF THE VELOCITY OF SOUND
IN WATER BY OPTICAL METHODS

by

Arthur Jared Crandall

A THESIS

Submitted to

Michigan State University

in partial fulfillment of the requirements

for the degree of

DOCTOR OF PHILOSOPHY

Department of Physics

1967

ACKNOWLEDGEMENTS

The author wishes to thank Professor E. A. Hiedemann for his guidance and patience. Throughout this work Dr. B. D. Cook gave valuable suggestions and provided many helpful discussions. Without the inspiration and help of Dr. F. Ingenito the theory section of this report would have been more complex and less exact. The financial support of this research by the Office of Naval Research and the National Science Foundation is gratefully acknowledged.

A.J.C.

TABLE OF CONTENTS

LIST OF FIGURES

LIST OF TABLES

LIST OF TABLES

I. INTRODUCTION

In spite of many measurements of the velocity of sound in water, made by various techniques, there is still no universally accepted value. Before the development of the piezoelectric transducer the measurements were generally confined to audible frequencies, which entailed propagation in a lake or ocean for free field results[1,2], or propagation in a closed pipe or Kundt's tube[3]. These early measurements were not satisfactory for the absolute determination of sound velocity because, in the first case, the physical parameters could not be accurately specified and, in the second case, the effect of confining the sound field was not accurately known.

With the development of the piezoelectric transducer and the associated electronics, continuous high frequency sound beams could be generated. With the possibility of many sound wavelengths in a small volume, Hubbard and Loomis[4] developed an interferometric technique for measuring sound velocities in liquids. This interferometer (based upon an interferometer designed by Pierce for measurements of sound velocities in air) consisted of a fixed quartz plate transducer and a movable, plane reflector. When the reflector is translated, standing wave resonances every half wavelength are indicated by variations in the transducer impedance. The interferometer, with many changes and improvements, achieved a great prominence for its high precision and small sample size.

TABLE 1. SOUND VELOCITY MEASUREMENTS* AT 30.00°C

NAME	DATE	METHOD	VELOCITY (m/sec)
Kundt and Lehman	1873	Kundt Tube	1040 to 1383
Hubbard and Loomis	1928	Interferometer	1509.9 ± 1
Schreuer	1939	Optical	$1509.6 \pm .2$
DelGrosso et. al.	1954	Interferometer	$1509.85 \pm .05$
Greenspan	1957	Time of flight	$1509.44 \pm .05$
Brooks	1960	Pulse	$1509.00 \pm .34$
Newbauer and Dragonette	1964	Pulse - freefield	$1509.00 \pm .20$
Ilgunas	1964	Interferometer	$1509.03 \pm .18$
McSkimin	1965	Phase Comparison	$1509.09 \pm .10$
DelGrosso	1966	Interferometer	$1509.11 \pm .02$

* These values were adjusted to 30.00°C using Greenspan's results.

The most carefully planned and analysed acoustic interferometer measurements were made by V. A. DelGrosso and his associates. His earlier measurements[5] agree quite favorably with the work of Hubbard and Loomis (see Table 1). The disagreement between these interferometer measurements and the pulse measurements by Greenspan (to be discussed later) is many times larger than the estimate of error for either measurement. This discrepancy led to several attempts to analyse the errors caused by diffraction. Recently, Ilgunas[6] and his co-workers obtained an empirical diffraction correction by operating their acoustic interferometer at several harmonics. They showed that diffraction effects raised the sound velocity values and the error decreased to negligible amounts as the frequency is increased. After an exhaustive theoretical investigation of diffraction and guided wave effects, DelGrosso[7,8,9] obtained an experimental value for the velocity of sound in water which is .74 m/sec lower than his previous measurements, and is closer to free field sound velocity measurements.

A second type of continuous wave measurement was developed by Bachem and Hiedemann[10-12] and later improved by Seifen[13] and Schreuer[14]. They used a parallel transducer-reflector configuration similar to an acoustic interferometer. However, they illuminated the standing wave sound field with a collimated light beam and observed the Fresnel interference pattern produced by the periodic phase modulation of the light. A velocity was determined by translating the sound field a large number of half wavelengths, as judged by counting the Fresnel interference fringes observed in a microscope, and measuring the sound frequency. The measurements of Schreuer were carried out over a frequency range of 2.4 to 10.8 mHz and show a general trend of lower velocities at higher frequencies - the measurements tend to approach an asymptotic value for frequencies above 7.2 mHz and are up to .6 m/sec higher at 2.4 mHz. This trend was probably caused by the diffraction and waveguide effects of the apparatus. The asymptotic value for the speed of sound in water is quoted in Table 1. Although diffraction effects were evident in Schreuer's work, the theoretical treatment of similar effects in the acoustical interferometer operating at short wavelengths (diameter $\gg \lambda$) was not completed until 1966 by DelGrosso[9]. Grabau[15] observed the equivalent behavior at long wavelengths (diameter $\sim \lambda$), as early as 1933, which led Grossmann[16,17] to a theoretical investigation of this behavior in 1934.

The second world war provided the impetus for sonar and radar development which consequently brought both increased need for accurate sound velocity measurements and sophisticated pulse generating and receiving equipment. There are a great variety of pulse-type methods, but only three which may be considered milestones, will be described.

Of the three pulse-type measurements, Greenspan's[18] National Bureau of Standards time coincidence pulse measurements are perhaps the most useful. The apparatus consisted of a 200 mm long steel tube terminated by transducers wrung on to the ends of the tube. His measurements are the first in which the sound velocity was measured over the entire 0° to $100^{\circ}C$ range with a method of very high precision. The resulting velocity versus temperature data for pure water are highly regarded by researchers[19,20] in the field and are used to compare results from measurements done at different temperatures. At a temperature of $30^{\circ}C$ he obtained a velocity 1509.44 $\pm$ .05 m/sec which is much lower than DelGrosso's earlier results but higher than his current results, by about .33m/sec. This difference is many times the specified probable error of either measurement.

In a 10 x 5 x 5 ft. cypress tank, Neubauer and Dragonette[21] performed an approximately free field measurement. A nearly spherical transducer radiated spherical wave pulses to a small probe-type transducer which could be positioned at accurately specified positions in the tank. The difference in time of arrival was measured for two probe positions colinear with the source. Unfortunately, tap water was used in the tank rather than distilled water and thermometry is somewhat more difficult in a big tank. However, if a correction for water impurity[18] is subtracted from their values, a pure water sound velocity of approximately 1509.0 $\pm$ .2 m/sec is obtained. This value is somewhat low compared to recent interferometer measurements but is very close to a similar measurement by Brooks[22] which, when a small free field diffraction correction[7] is applied also gives a pure water velocity of approximately 1509.0 $\pm$ .3 m/sec.

The last pulse type measurement to be described was done by McSkimin[20,23] at Bell Telephone Laboratories. His physical arrangement consisted of two precisely ground and polished fused silica buffer rods separated by a fused silica spacer ring which formed the sample cavity. A pulsed continuous wave is generated by a 20 mHz fundamental frequency transducer mounted on the end of the fused silica buffer rod. The wave is then interrupted and the echoes are observed on an oscilloscope. Interference effects from overlapping echoes allow the adjustment of the wave frequency so that an integral number of wavelengths occur in the cavity formed by the spacer ring. The adjustment of the wave frequency,which yields results of high precision, is very critical. However, the length of the spacer ring was, at most, 12.7 mm, which when measured even with the best comparator, placed a definite upper limit upon the overall accuracy possible ($\sim 1:10^5$). Also, mercury-in-glass thermometers, which are generally less satisfactory for absolute temperature measurement, were used. These measurements were carried out over a temperature range of 20°C to 75°C. Comparison which Greenspan's measurements show an essentially constant difference of .36 m/sec over the entire temperature range. The sound velocity versus temperature curve is parabolic with a maximum around 74°C. Since the difference between the measurements of Greenspan and McSkimin is constant,and not temperature dependent, thermometry is eliminated as a potential cause of this difference. McSkimin obtained a sound velocity in pure water which compares very favorably with DelGrosso's later results and is only about .1 m/sec higher than the corrected free field results of Neubauer and Dragonette and those of Brooks.

Other references[5,24,25] describe a great many more techniques for the measurement of sound velocities; these will not be discussed in this thesis.

With this large group of carefully planned and executed experiments, and the differences and agreements which exist among them, a desire was expressed at the seventy-first meeting of the Acoustical Society of America for a new, independent method of measuring the velocity of sound. With the extended experience of optical methods for the investigation of acoustical fields here at Michigan State University, it was an easy and natural step to undertake another investigation of sound velocity measurement by optical methods. In the thirty years since Schreuer's investigation, new equipment such as the laser, pulse generating equipment, and a fast response photomultiplier permits the development of new optical methods. In fact, three new methods were devised, continuous progressive wave measurement, pulsed continuous wave measurement and pulsed phase comparison measurement. Also, with this new equipment Schreuer's experiments could be repeated at considerably lower sound pressures, which means that the heating effects which were not negligible in Schreuer's work were greatly reduced in the present work.

II. DESCRIPTION OF EXPERIMENTS

Bachem, Hiedemann and Asbach[26] and Nomoto[27] have shown that when a collimated beam of light passes through a stationary ultrasonic wave, the wavefronts of the sound wave may be made visible. The stationary sound beam consists of condensations and rarefractions which cause a periodic change in the index of refraction of the medium. As the plane light wave passes through the sound beam those parts which pass through condensations become retarded in phase relative to the parts which pass through rarefractions. As the light wave moves further away from the sound beam, the phase modulation produces an amplitude modulation which may be seen with a ground glass or a microscope. This is called a "visibility pattern" and results from "secondary interference". This visibility pattern, as viewed by the eye, does not move in the direction of the sound wave because the acoustic wave producing it is stationary.

For the case of a progressive wave or pulse, the visibility pattern moves with the sound wave, like a shadow. This will be described in a more mathematically satisfying manner in the Theory section of this report. One could use a Kerr-cell stroboscope, as Bachem did, to "stop" the motion. However, a photomultiplier capable of responding to magacycle signals is a valuable alternative because it permits an oscilloscope display of these variations in light intensity.

The continuous wave and standing wave measurements were made with the apparatus shown schematically in Fig. 1. The photomultiplier converted the fluctuating light intensity to an electrical signal which was amplified by a series of three wide band amplifiers. From the output of the amplifiers, the electrical signal was connected to the vertical input of the oscilloscope. The rf power, generated by the transmitter, was distributed by the matching circuit to the transducer and to the horizontal plates of the oscilloscope. The phase of these two signals was compared using the resulting Lissajous pattern. The experiment then consisted of observing the Lissajous pattern on the oscilloscope while translating the transducer. The translation was measured for an integral number of wavelengths.

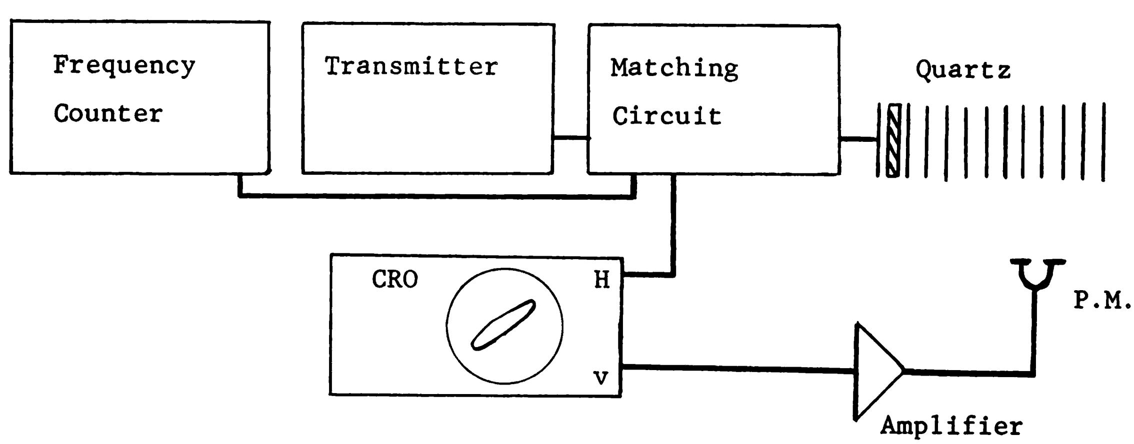

Figure 1. Standing Wave and Progressive Wave Block Diagram.

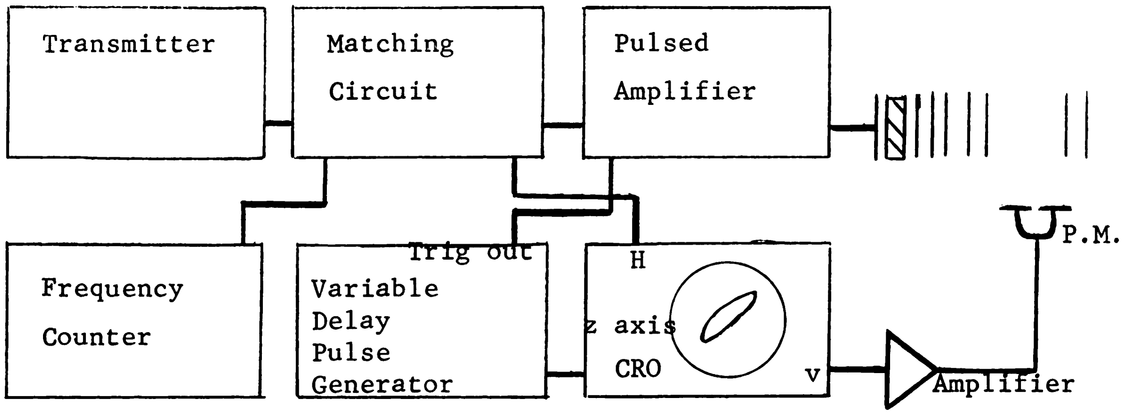

Figure 2. Pulsed Progressive Wave Block Diagram.

The circuit for pulsed continuous wave measurement is shown in Fig. 2. The transmitting circuit now includes a pulsed amplifier which generates a ten microsecond pulse every 1/60th of a second. The photomultiplier circuit is identical to that in the previous discription. Finally, in order to observe only the effect of the pulse, a suitably delayed square wave from a Dumont pulse generator modulates the oscilloscope intensity (z axis). Thus the oscilloscope trace appeared only when the sound pulse traversed the light beam. The measurements were carried out in the same way as the continuous wave measurements except that as the transducer was translated, the delay in the oscilloscope modulating pulse was also changed.

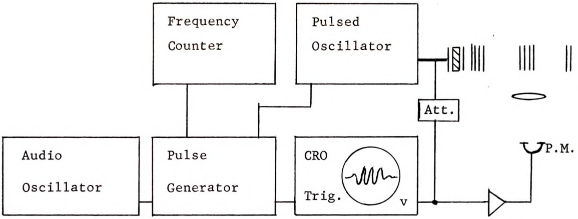

Figure 3. Pulsed Time Coincidence Block Diagram.

The pulsed time coincidence measurement is an attempt to do a measurement somewhat similar to that of Greenspan. The pulses of 1 microsecond pulse length and a center frequency of 6 mHz are generated by the Arenberg pulsed oscillator and the related equipment (Fig. 3). The pulse repetition rate is 50 kHz and is controlled by the audio oscillator. The spacing of the acoustical pulses in the tank is, of course, proportional to the sound velocity and, for the repetition rate used, was about 30 mm. A different optical system was used; the laser beam was focused upon the acoustical axis, making a very narrow light beam at the position of the sound beam. A second lens focused the laser beam on the photomultiplier. The sound deflects the light beam approximately sinusoidally about its mean position so that a train of nearly sinusoidal waves was displayed on the oscilloscope.

A regular horizontal sweep was used on the oscilloscope which then displayed the oscillations in the optical signal when one of the pulses crossed the light beam. A small amount of the signal applied to the transducer was also fed to the vertical oscilloscope input through an attenuator. A measurement was made by first superimposing the transducer voltage pulse and the optical signal pulse, and then translating the transducer until another optical pulse was superimposed. The distance translated, multiplied by the repetition frequency, gives the sound velocity.

Diffraction has been mentioned as a possible source of errors in sound speed measurements. To illustrate one effect of diffraction, a zeroth order schlieren photograph of the sound field of a 2 mHz transducer of radius 11 mm is shown in Fig. 4. The complicated pattern of light and dark areas is a direct result of the non-uniformities in the sound field which are caused by diffraction. For the case of a progressive wave, the effect of diffraction on optical sound velocity measurements has heretofore been treated neither experimentally nor theoretically. The next section will be devoted to this problem.

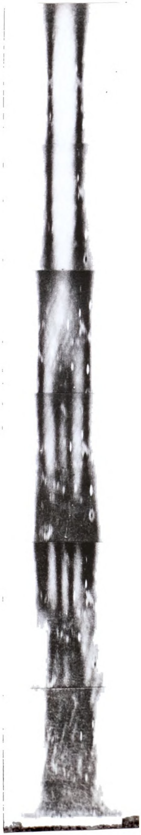

Figure 4. Zeroth Order Schlieren Photograph of a Sound Beam Radiating from a 2 mHz, 22 mm dia, Transducer.

THEORY

In order to examine the effects of diffraction on optical sound velocity measurements, an expression for the sound field will be developed. Next, the effect of the sound field on the light beam will be calculated. Here we will assume that the light beam is not deviated as it passes through the sound field; therefore, only the relative retardation in phase of the light beam (retardation v, for short) is calculated. This is equivalent to the Raman-Nath approximation. And finally, the light intensity measured at the photomultiplier is derived from the expression of the retardation of the light beam.

A circular transducer of radius a, is mounted in an infinite rigid baffle on the x-y plane (Fig. 5). The transducer vibrates sinusoidally with angular frequency ω into a linear, dissipationless fluid. The resulting sound field may conveniently be described by the velocity potential φ, in terms of which, the particle velocity u and pressure p may be calculated from the equations

$$u = - \nabla \varphi \tag{1}$$

and

$$p = \rho_o \dot{\varphi} , \tag{2}$$

where ρ_o is the density of the medium. With the time dependence $e^{-i\omega t}$ understood, the velocity potential satisfies the Helmholtz equation

$$\nabla^2\varphi + k^2\varphi = 0, \tag{3}$$

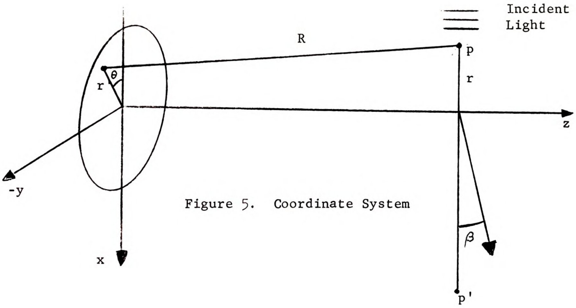

Figure 5. Coordinate System

where $k = \omega/c$ and c is the velocity of sound in the fluid. The boundary condition on φ is

$$-\left.\frac{\partial\varphi}{\partial z}\right|_{z=0} = \begin{cases} f(r') , & r' \leq a \\ 0 , & r' > a \end{cases} \tag{4}$$

where $f(r')$, the velocity normal to the transducer, is considered to be a known function of r' only.

The velocity potential satisfying Eqs. (3) and (4) may be expressed in several equivalent ways. In our calculations we will use Rayleigh's expression[28]

$$\varphi(P) = \frac{2\pi}{ik} \int_s f(r') \frac{e^{-ikR}}{R} r'dr', \tag{5}$$

and also the expression of Bateman[29] and King[30]

$$\varphi(P) = \int_0^\infty e^{-\mu z} J_o(\alpha r) g(\alpha) \frac{\alpha}{\mu} d\alpha, \tag{6}$$

where $$R = (z^2 + r^2 + r'^2 - 2rr'\cos\theta)^{1/2},$$

$$\mu = (\alpha^2 - k^2)^{1/2}, \text{ and}$$

$$g(\alpha) = \int_0^a f(r') J_o(\alpha r') dr', \tag{7}$$

where J_o is the zeroth order Bessel Function.

If the transducer vibrates with uniform velocity u_o over its surface, the function $f(r')$ equals u_o, so that Eq. (5) becomes

$$\varphi(P) = \frac{2\pi u_o}{ik} \int_0^a \frac{e^{-ikR}}{R} r'dr'. \tag{8}$$

By substituting $f(r') = u_o$ in Eq. (7) and integrating, an expression for $g(\alpha)$ may be obtained, which when substituted in Eq. (6) gives the velocity potential

$$\varphi = au_o \int_0^\infty e^{-\mu z} J_o(\alpha r) J_1(\alpha a) \frac{d\alpha}{\mu}. \tag{9}$$

Later, some results obtained from these expressions for the velocity potential will be discussed.

Now that expressions for the sound field have been obtained, the retardation v of the incident plane wave of light may be calculated. Consider the light beam to be traveling parallel to the x axis in the x-z plane so that it passes through the diameter of the sound beam. Then, if n is the index of refraction and s the entropy, the axial retardation is expressed as

$$v_a = \frac{dn}{dp}_s k' \int_{-\infty}^{\infty} p \, dx \quad . \tag{10}$$

Combining Eqs. (2), (9), (10) the expression for the retardation becomes

$$v_a = \frac{dn}{dp}_s k' i\omega\rho_o\mu_o a e^{-i\omega t} \int_o^{\infty} \frac{e^{-\mu z}}{\mu s} J_1(\alpha a) \left[\int_{-\infty}^{\infty} J_o(\alpha r) dx\right] d\alpha$$

$$= [\text{constant}] \; e^{-i\omega t} \int_o^{\infty} \frac{e^{-\mu z}}{\mu} \, 2 \, \frac{J_1(\alpha a)}{\alpha a} \, d\alpha \tag{11}$$

Using the identity $2 J_1(\alpha a)/(\alpha a) = J_o(\alpha a) + J_2(\alpha a)$ and the integral *

$$\int_o^{\infty} \frac{e^{-\mu z}}{\mu} J_n(\alpha a) \, d\alpha = \frac{\lambda\pi}{2} \left[H_{n/2}^{(1)} (B) \, J_{n/2} (A)\right], \tag{12}$$

where $A = \frac{k}{2} [\sqrt{z^2 + a^2} - z]$, and $B = \frac{k}{2} [\sqrt{z^2 + a^2} + z]$,

the retardation may be expressed as

$$v_a = \frac{\pi}{2} \frac{dn}{dp}_s k' \omega\rho_o\mu_o a e^{-i\omega t} \left[J_o(A) \, H_o^{(1)} (B) + J_1(A) \, H_1^{(1)} (B)\right], \tag{13}$$

This expression involves only well-tabulated Bessel and Hankel functions. By taking the imaginary part of v_a (this is equivalent to assuming that the transducer vibrates with $\sin(-\omega t)$ time dependence) the

- - - - - -- -

* F. Ingenito, private communication.

retardation v_a may be expressed in the form

$$v_a = v_o(z) \sin(kz - \omega t + \theta(z)), \tag{14}$$

where

$$v_o(z) = |v| = [(Re v_a)^2 + (I_m v_a)^2]^{1/2},$$

and

$$\theta(z) = \tan^{-1} [(I_m v_a)/(Re v_a)] - kz + \omega t \quad .$$

With the optical retardation expressed in Eq. (14), there remains the question: "What does a photomultiplier light detector see when placed some distance x from the sound beam along the path of the laser beam?" The approach to the solution will be to first note from Eq. (14) that the light beam has a nearly periodic variation in phase as it emerges from the sound beam; this variation in phase directs the light into diffraction orders. And finally from light travelling in these orders, a Fresnel diffraction pattern will be calculated for the experimental conditions at hand.

Numerical analysis of Eq. (14) indicates that the amplitude and relative phase of the retardation v oscillate rapidly near the transducer but their rate of oscillation decreases until at approximately $\frac{z\lambda}{a^2} > .3$, they may be considered slowly varying functions of z. Therefore, the retardation may be expressed as

$$v = v_o \sin(kz - \omega t + \theta_o) \tag{15}$$

where v_o and θ_o are slowly varying functions of z and may be considered constant over the width of the laser beam.

The diffraction integral expresses the amplitude of the light emerging in the direction β:

$$A(\beta) = C \int_L \exp \quad i[k'z\sin\beta + v_o \sin(kz-\omega t + \theta_o)] \ dz \qquad (16)$$

where k' is the wave number of the light and C is a complex constant. Inserting the identity

$$\exp [iv\sin \varphi] = \sum_{n=-\infty}^{\infty} Jn(v) \exp [in \varphi] \qquad (17)$$

in Eq. (15), the amplitude may be expressed as:

$$A(\beta) = C \int_L \exp [i\ k'z\sin\beta] \sum_{n=-\infty}^{\infty} Jn(v_o) \exp [in(kz-\omega t + \theta_o)] \ dz$$

$$= C \sum_n Jn(v_o) \exp [in(-\omega t + \theta_o)] \int_L \exp [iz\ (k'\sin\beta + nk)] \ dz. \qquad (18)$$

If the light beam has infinite width, the integral predicts discrete diffraction orders at angles β_n where $\sin \beta_n = nk/k'$. In the measurements to be described later, the light beam was from two to ten wavelengths wide. Consequently this integral predicts diffraction orders which are somewhat smeared out.

However, if one assumes that the orders are discrete, the Fresnel field may be easily calculated[31]. The diffraction orders may be considered to be plane waves traveling in directions β_n with amplitudes

$$A_n = J_n(v_o) \exp [in(-\omega t + \theta_o)] \ , \qquad (19)$$

which may be added at the position of the photomultiplier.

Thus the amplitude in the Fresnel field is given by

$$A(z,x) = \exp\,[-ikx] \sum_n J_n(v_o) \exp\,[in\,\delta] \exp\,[-in^2 qx] \qquad (20)$$

where

$$\delta = kz - \omega t + \theta_o \quad \text{and } q = \frac{k^2}{2k'} \text{ .}$$

In the measurement of sound velocity, local heating and finite amplitude effects although small, may cause errors. For this reason the transducer potential is adjusted to give a small but measurable optical effect. This restriction held $v_o \sim 0.1$ so that $J_1(.1) \ll 1$ and $J_2(.1) \ll J_1(.1)$. Therefore, the approximate light intensity may be calculated very simply:

$$A(x,z) = J_o(v_o) + 2iJ_1(v_o) \sin\delta \exp\,[-iqx]. \qquad (21)$$

And thus, the intensity may be expressed as

$$I = AA^* = J_o^2(v_o) + 4\, J_1^2(v_o) \sin^2\delta + 4J_o(v_oJ_1(v_o) \sin\delta\sin qx$$

or by taking the first term in the Taylor series expansion for $J_n(v_o)$, as

$$I = 1 + 2v_o \sin\delta \sin qx \text{ .} \qquad (22)$$

This simple approximation shows several important features of the Fresnel interference pattern. Remember that the relative retardation was $v_o \sin\delta$; the fluctuating part of the intensity is exactly in phase with the relative retardation. In this approximation the intensity modulation is proportional to the transducer voltage and the distance from the sound beam. A more complete analysis[32] would show more complicated relationships at higher sound intensities; however, the first prominent intensity peak is at $\delta = \pi/2$ for various values of retardation and at various positions from the transducer as long as $q\, x < 0.2$. This means that the phase relationship between the transducer voltage (proportional to v) and the light intensity at the photomultiplier is constant for a given z position, independent of the magnitude of the transducer voltage.

IV. THEORETICAL RESULTS

The mathematical connections between the velocity distribution at the transducer, the sound pressure at any point in the sound field, and the intensity of the light beam at the photomultiplier have been established. Now, from the theory, some calculations are presented which will point out some features of typical sound beams. Special attention will be given to those features which influence the accuracy of sound velocity measurements. The discussion will parallel the order followed in the preceeding section, that is, first the velocity potential is considered, which gives the spatial pressure distribution, then the optical effects are described.

From the theoretical work of Meixner[33], Seki et al[34], DelGrosso[5], Williams[35] and the early experimental work of Hiedemann and Osterhammel[36-38], a picture of the sound field has evolved. The sound field of a transducer whose diameter is many wavelengths, is very complicated, having some curvature of wavefronts and a very complex variation of pressure.

In order to carry out a complete, although approximate calculation of a sound field and the resulting optical effect, a numerical evaluation of Eq. (6) was done with a CDC 3600 computer. First, to be discussed here, the program calculated the pressure and phase of the near field of a transducer of 5 wavelength radius. This transducer radius was chosen so that the computer time could be minimized, as well as approximating experimental conditions.

This calculation was simply performed by dividing the transducer area into small squares (1/3 λ) and summing the effects at the observation points. To check the computer program, the axial pressure was plotted in Fig. 6 and compared to the well known exact integral. The agreement between curves could be improved by dividing the transducer into smaller squares.

The nature of this curve, with its characteristic axial nulls, serves as a "precursor" of the optical results to be discussed later on.

The calculated pressure distribution is shown in Fig. 7. Note that there is appreciable pressure amplitude for r greater than the transducer radius, which indicates a poorly collimated sound beam. For the transducers and frequencies used in this experiment, the collimation is somewhat better because $r > 8\lambda$. The development of side lobes is also evident in this figure. The phase, or the wave fronts, are plotted in Figure 8. Note that the approximation to a plane wave is not very good - especially on the axis where there are the characteristic dimples. For r greater than the transducer radius, the wavefronts are strongly curved. When a light beam traverses a sound beam, it essentially integrates over the pressure distribution along its path; when passing through these strongly curved wavefronts, the rapidly varying phase tends to nullify the effect of the pressure amplitude outside the cylinder whose base is the transducer.

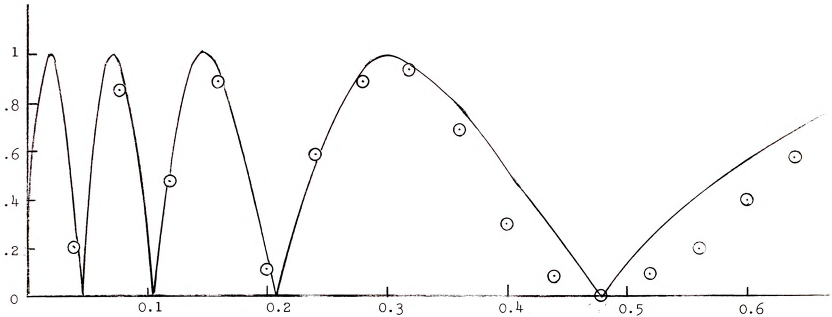

Figure 6. Axial Pressure a = 57

⊙ computer calculation

—— $\left| \sin \frac{k}{2} (z^2 + a^2 - z) \right|$

For light passing through the center of a sound beam, the retardation is given by the exact expression in Eq. (13). The amplitude of this retardation is plotted in Fig. 9 for the same transducer radius to wavelength ratio as the previous graphs. The effect of the strong oscillations of the axial pressure can be clearly seen. Although, because of the light beam's averaging effect, the oscillations are greatly suppressed. The maximum retardation occurs at $\frac{z\lambda}{a^2}$ 1.1 and not at the transducer as one might assume. The most important result suggested by this curve is that the exact effect of the near field on transducer pressure calibration by optical methods is now specified.

Since a light beam has finite dimensions, the resulting light diffraction is from light which passes through the sound beam somewhat off axis. In order to investigate the contribution of this off axis light, the same computer program, using the pressures already calculated, performed this optical integration numerically. With the solid curve being the exact solution, Fig. 10 shows the results of these computer calculations. The agreement between the exact solution and the computer solution for the integration through the diameter is better than might be expected. The various off-axis retardation values tend to oscillate with smaller amplitude. With a finite sized light beam of 2 sound wavelengths in diameter, for example, the optical effect would be similar to Fig. 9 but with less variation in amplitude.

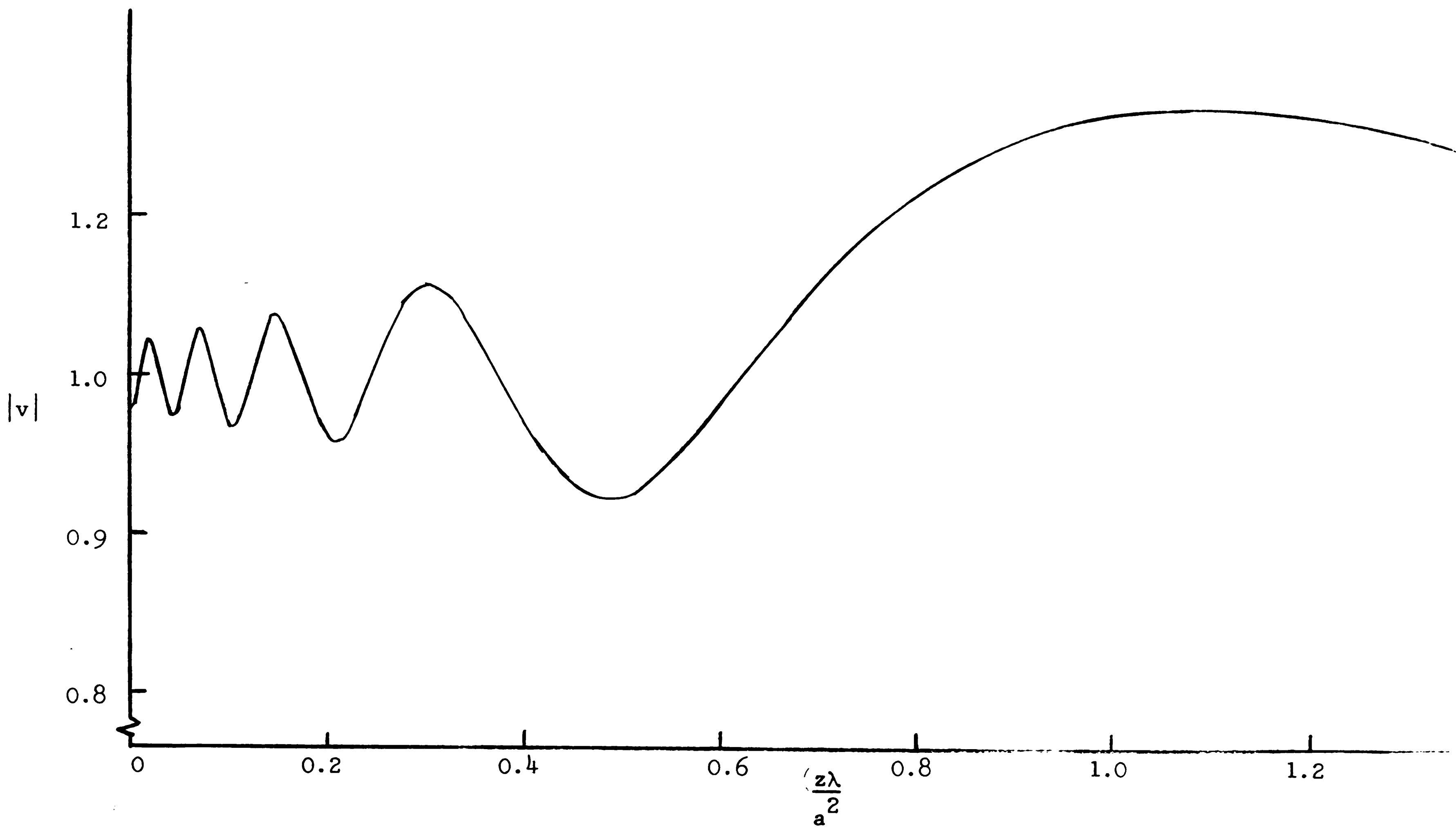

Figure 9. Relative Retardation Integrated along Sound Beam Diameter $a = 5\lambda$.

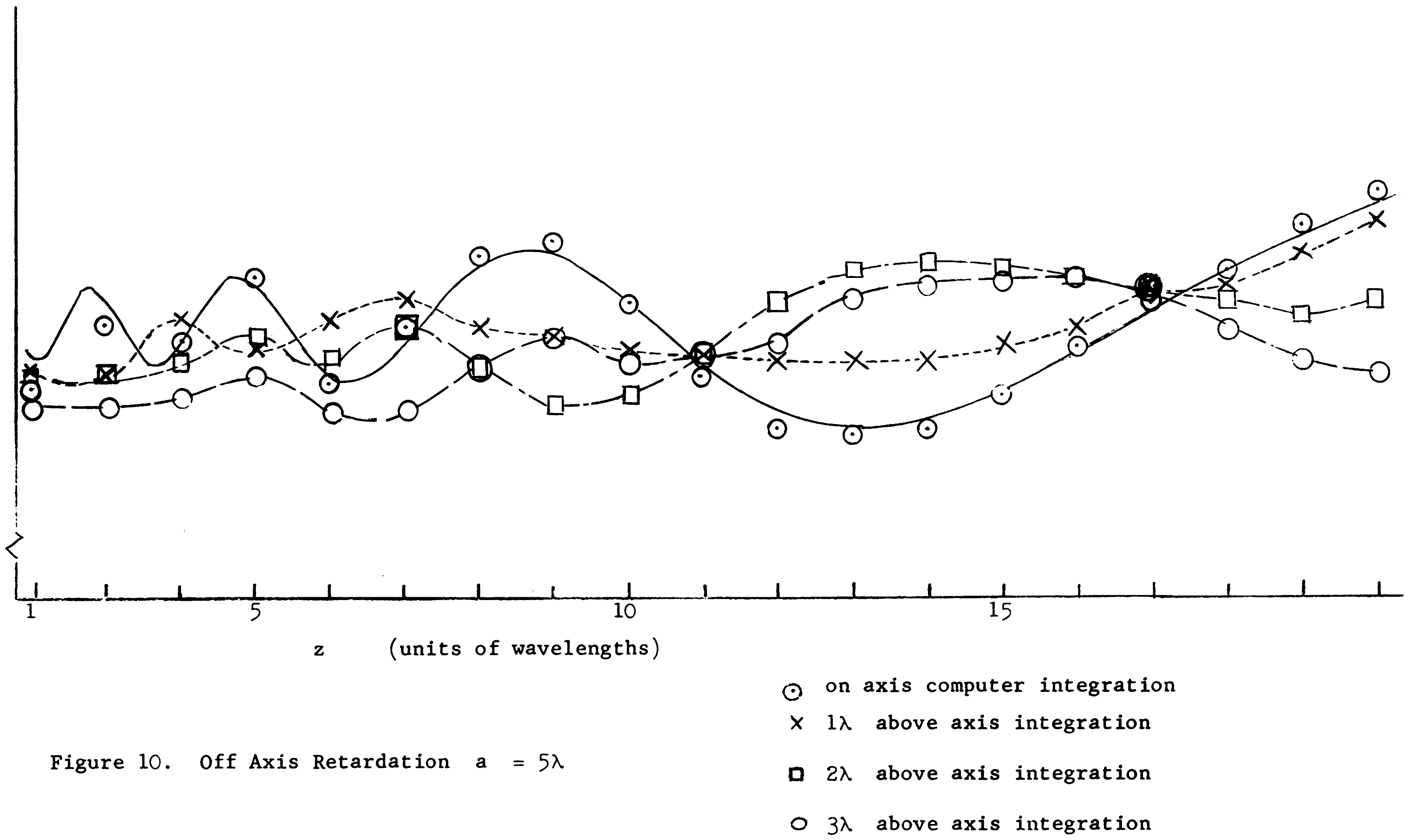

Figure 10. Off Axis Retardation a = 5λ

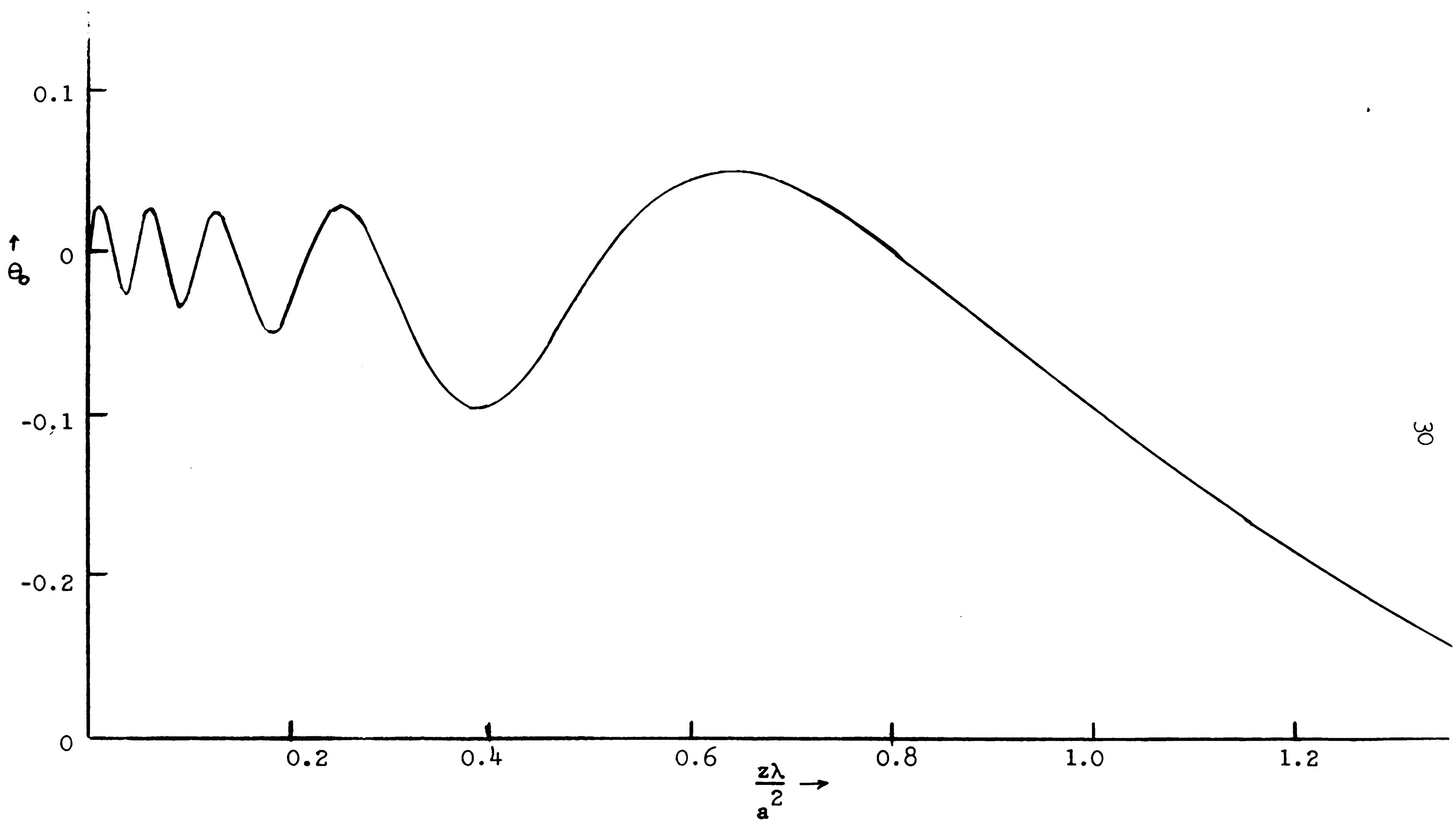

Figure 11. Relative Axial Optical Phase $a = 5\lambda$.

The curve of the phase of the retardation, relative to the plane wave phase, is plotted in Fig. 11. For a/λ ratios greater than 5, the curves are found to be similar to the one shown except that in the region $z\lambda/a^2 < .8$ there are more oscillations. Since the light intensity at the photomultiplier has been shown to be proportional to the retardation for low sound intensities, the phase of the electrical signal from the photomultiplier equals the phase of the retardation plus some constant phase shift due to the electronic circuits.

Using the signal applied to the transducer as a phase reference, a Lissajous pattern on an oscilloscope indicates the phase of the signal voltage relative to the phase of the photomultiplier output. Since phases are compared, the amplitude of the retardation is unimportant if the electronic circuits are linear.

A sound velocity measurement might be carried out in this way: the transducer is translated until the value of z is such that a Lissajous pattern is closed; next the transducer is moved a whole number of wavelengths indicated by the Lissajous pattern again being similarly closed. By measuring the distance translated, the wavelength is measured, and finally the velocity computed. If the phase θ_o [Eq. (14) $v = v_o \sin(\omega t - kz + \theta_o)$] was a constant over the range of measurement, then such a measurement would give the true plane wave phase velocity c sinde $k = \omega/c$. However, measurements are usually made over a large number of wavelengths to increase the precision. Therefore, the fact that θ_o is a slowly varying function of a z introduces a systematic error in the sound velocity measurement.

Because the value of θ_o is know as a function of z, the distance from the transducer, including this correction will eliminate this systematic error from the absolute error. The correction is introduced in the following way: At position 1 the spatial phase of the argument in Eq. 14 becomes $kz_1 + \theta_{o1} = 2\pi m_1$, when the Lissajous figure is closed; in the same manner, at position 2 the phase is $+ kz_2 + \theta_{o2} = +2\pi m_o$ where the difference between n_1 and n_2 is the integral number of wavelengths measured. Then the velocity is calculated from these two equations giving

$$c = \frac{\omega\Delta z}{2\pi\Delta n + \Delta\theta_o} \qquad (21) \qquad \text{where } \Delta z = z_1 - z_2 \text{ etc.}$$

For instance, in Fig. 11 if the measurement was carried out for $z_1\lambda/a^2 = 1.2$ and $z_2\lambda/a_2 = 0.8$ the corresponding phases would be $\theta_{o1} = 0.182$ and $\theta_{o2} = + 0.005$. Thus the measured velocity $\omega\Delta z/2\pi\Delta n$ would be higher than the plane wave value c, by approximately $\frac{-\Delta\theta}{2\pi\Delta n} = 0.3\%$. However, if a measurement was made between $z_1\lambda/a^2 = 0.8$ and $z_2\lambda/a^2 = 0$, for instance, $\Delta\theta = + .01$ the measured velocity would be lower than the plane wave phase velocity "c" by an amount less than .01%.

To sum up these results, when the optical phase curve $\theta_o(z)$ is known for a given transducer geometry, the effects of diffraction on the measurements of the sound velocity may be calculated and the measurements thus corrected to give the plane wave phase velocity "c". Furthermore, this correction is valid for all distances from the transducer.

V. DESCRIPTION OF EQUIPMENT

This chapter contains a description of the equipment used in the experiments described in chapter II. A diagram of the optical bench is shown in Fig. 12. A stable optical system is required for the measurements described here. The optical bench was constructed of oak, bolted and glued in bulkhead type configuration. Supports (not shown) for the tank of water and the lathe bed were built in triangular form for rigidity.

The light source was a He-Ne laser (Spectra Physics 131) which has a collimated beam of high intensity radiating from the front and a slightly diverging weaker beam from the back. The laser was firmly mounted on an optical rail fastened to the bench. All other optical parts, including the windows of the tank, were aligned to the primary beam of the laser. Light from the rear of the laser, directed by three right angle prisms, illuminated a Michelson interferometer used for the length measurement.

The photomultiplier was located behind the tank 20 to 50 cm from the sound beam, depending on the frequency. Although the photomultiplier tube 1P21 has an s-4 surface which is not particularly sensitive to the red line of the He-Ne laser, the sensitivity was adequate. The output impedance of the photomultiplier was controlled to obtain maximum signal response for the bandwidth required. A further description of the photomultiplier can be found elsewhere[31].

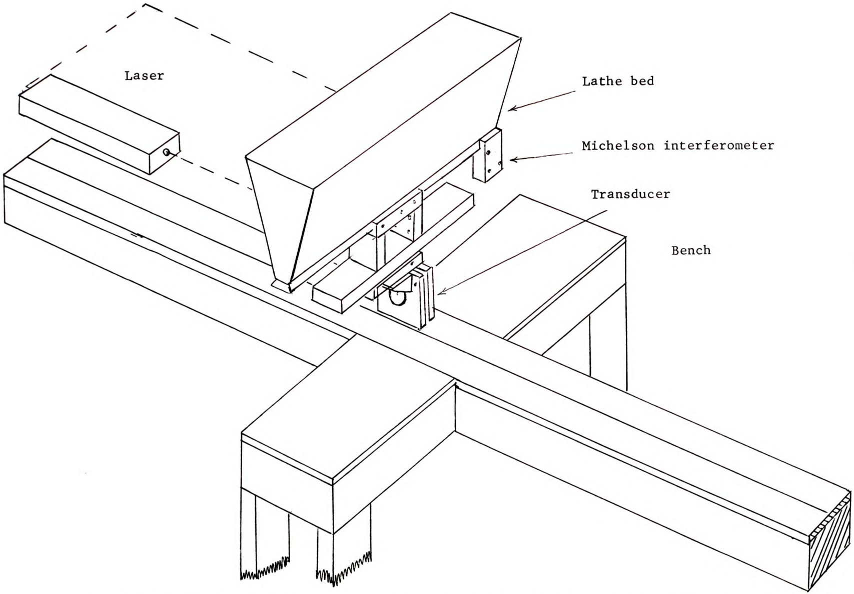

Figure 12. Optical Bench and Transducer Mounting (overhead supports not shown)

Unlike Schreuer's arrangement, which moved the entire tank and transducer assembly, only the transducer was moved in this experiment. Thus, any curvature or imperfections in the tank windows (carefully chosen and mounted optical flats) will not effect the measurements.

In these sound velocity measurements, the translation of the transducer must be measured to the accuracy desired for the velocity measurement. In addition to accuracy, the problems of precision, convenience, and finance must be considered.

The transducer mount was attached to the carriage of a miniature lathe bed. A screw, which could be turned either by motor or by hand, drove the carriage along the dovetail guide of the lathe bed. At one end of this guide, the beam splitter and fixed mirror of a Michelson interferometer were attached. The moveable mirror was attached to the carriage on the lathe bed. The illuminating light for the interferometer came from the laser as previously described. The fringe system was monitored by a photomultiplier tube which was also mounted on the dovetail guide.

As the transducer assembly is moved, the interferometer photomultiplier produces pulses in accordance with the detected fringe pattern. This output was amplified and shaped into uniform pulses to insure consistent counting by a Beckman scalar. It is recalled that a Lissajous pattern on an oscilloscope indicates the relative phase between the optical effect and the driving signal. With a motor moving the transducer at a nearly uniform rate, the scaler was switched on at one closing

of the Lissajous pattern and switched off at another, similar closing of the pattern. Thus the count of the fringes yields a length measured for an integral number of wavelengths of sound. The major advantage of this type of measurement is that it is an absolute length measurement because it depends only upon the wavelength of the He-Ne laser line (6328.17 A). The disadvantage is that the measurement takes a great deal of time and the precision of the starting and stopping is not high enough to obtain satisfactory statistics without many tedious repetitions.

To crosscheck and to expedite the length measurement, an alternate system, using Johannasen gage blocks was used. Fastened to the other end of the dovetail guide, a Browne and Sharpe micrometer screw, calibrated to $\pm$ .002 mm, was mounted in a sturdy aluminum block. Gage blocks could be inserted between the micrometer screw and the transducer mount. The micrometer screw was then used to interpolate between gage blocks. With a Sheffield comparator, Fonda ($\pm$ .2 microns) gage blocks, which had been recently calibrated, were used to calibrate the working set of gage blocks.

The Michelson interferometer also provided a good check of the trueness of the dovetail guide. The circular fringe pattern is very sensitive to angular displacements of the movable mirror which follows the angular deviations of the motion of the transducer carriage. Since the fringe pattern remained centered over the measurement range used, the transducer motion was assumed to be only a translation with no angular deviation.

In the continuous progressive and standing wave measurements, the rf potential applied to the transducers was generated by a 100 watt transmitter. In the pulse measurements, two Arenberg model 650PG pulse units were used; One operated at a pulsed oscillator and the other as a gated amplifier of the signals from the rf transmitter. The gated amplifier was triggered by a Dumont 404R generator. The frequency of the transmitter was monitored by a Hewlett Packard 524 B frequency counter. Its standard frequency, accurate to $1 : 10^6$, was checked against a more accurate laboratory standard (Hewlett Packard .5245L).

The sound was generated by x-cut quartz transducers which were mounted with air-backing in holders of nylon. The transducer was aligned perpendicular to the light beam prior to each set of measurements. To permit angular adjustments in the transducer orientation, the holders were constructed with gimbal pivots for the horizontal rotation and knife edge pivots for the vertical rotation.

A transducer of similar construction was used as the reflector in the standing wave measurements. The air backing of the quartz gave the standing wave cavity a very high "Q" so that the required driving potential was on the order of 5 volts.

One important disadvantage of previous optical methods is that large acoustical pressures were required to produce an observable effect. The eventual dissipation of the acoustical energy within a resonant cavity resulted in the local heating of the medium. Schreuer, for example, found that his measurements of sound velocity in water were raised as much as 0.6 m/sec at his highest acoustic power levels. In an attempt to account for this local heating, the sound velocity was measured at several acoustic power levels and the results extropolated to a value for zero acoustic power.

The sound velocity in water at room temperature changes by approximately 3 m/sec per degree centigrade; therefore, temperature changes of .01 degree centigrade are significant. Considerable thought was devoted to the design of the present arrangement to insure that:

a) minimum acoustical energy was dissipated in region of measurement;

b) heating from the energy dissipated in the transducer was not significant;

c) absolute temperature was measured in a region in proximity with sound beam;

d) temperature variations in the tank were minimized by adequate stirring and pumping of the medium; and yet

e) adequate flexibility was available to allow different configurations.

A diagram of the resultant experimental arrangement is shown in Fig. 13. The tank (15 cm x 15 cm x 80 cm) is constructed of aluminium and is insulated on the sides, bottom and partially on the top with a 4 cm layer of styrofoam. The best location of the temperature control elements, determined by trial and error, is shown in Fig. 13. A pump circulates the water through a chamber containing an immersion

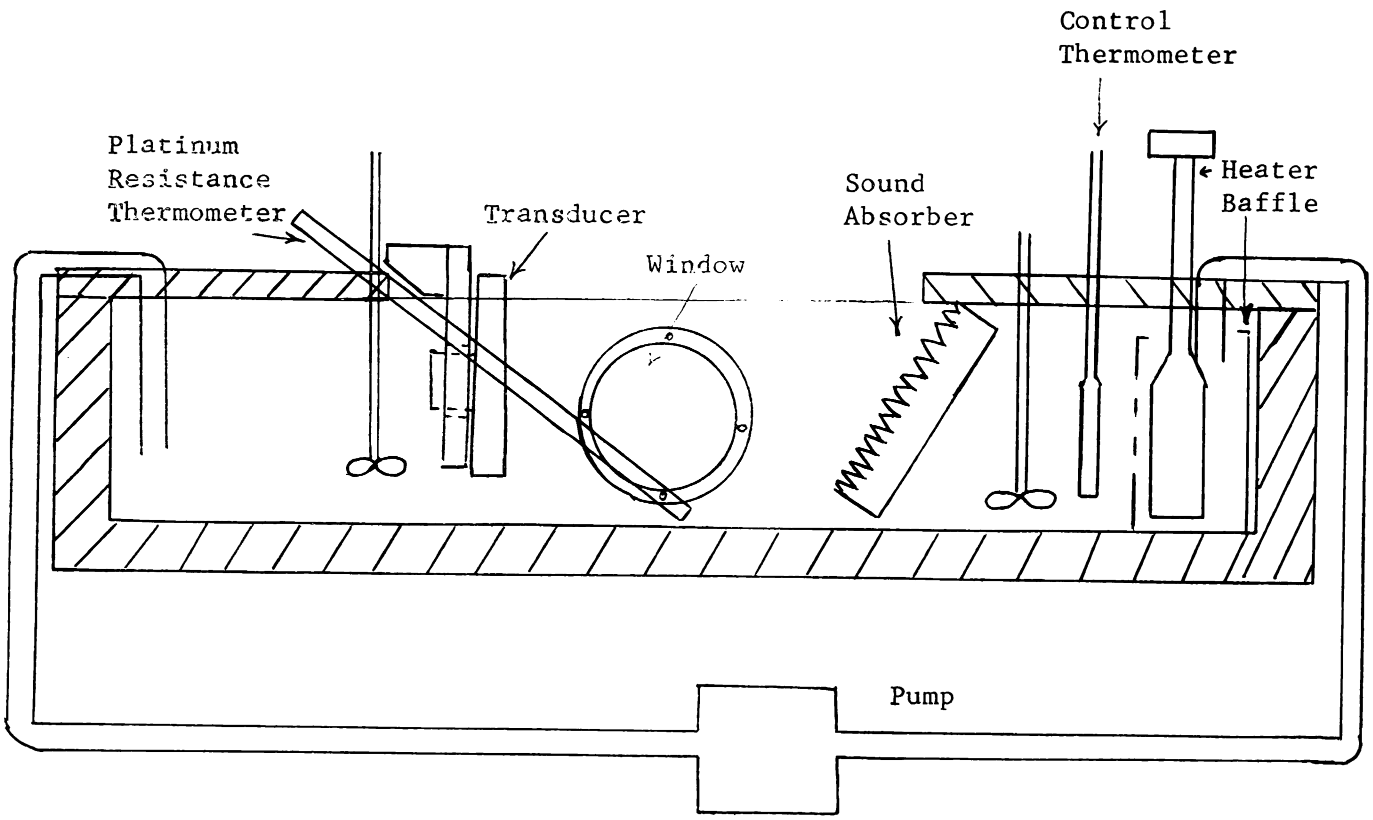

Figure 13. Tank and Temperature Control

heater. Then the water flows past the control thermometer of a Bayley Instrument Company proportional controller which controls the heater power. Next, the water flows around the sound absorber and through the measurement area. In this area, the water is also stirred by one or two stirrers, depending on transducer configuration, to insure temperature uniformity. By working at approximately ten degrees above room temperature, no auxiliary cooling device was required. The temperature uniformity was investigated for a variety of conditions with a pair of thermocouples and a Kiethly micro-voltmeter Model 149. The reference junction was placed in a water-filled flask which was placed in the measurement tank. The other junction, fastened to the end of a glass rod, was used to probe temperature differences.

With the temperature control apparatus turned off, and the water not circulating, the temperature variation was about $.02^{\circ}C$. With temperature control apparatus operating and the water pumped and stirred, the maximum temperature variation over the entire tank was less than $.01^{\circ}C$. In the space where the measurements were made, the temperature variation was at most $.005^{\circ}C$.

Next, the temperature variations produced by the sound beam and the heat dissipation of the transducer were investigated. In order to achieve a significant temperature change, a high input of rf power (70 watts at 300 v) was applied to the transducer. The temperature of water at the surface of the transducer increased about $0.2^{\circ}C$ above the ambient temperature of the tank. At one centimeter from the transducer the increase was only $.05^{\circ}C$. For progressive wave and pulsed progressive wave measurements the rf potential applied to the transducer was at most one fifth the potential applied in this test; for standing waves the applied potential was less than one sixtieth of the test value. Consequently, the temperature variations should be reduced by the order of 10^{-2} to 10^{-4} of the temperature variation given above.

The absolute temperature was obtained by placing a platinum resistance thermometer adjacent to the sound field. With adequate stirring, the temperature difference between the sound field and thermometer was negligible. The resistance of the platinum resistance thermometer (Radio Frequency Labs) was ascertained using a Mueller bridge (Leeds and Northrup type 01). This bridge was calibrated at room temperature using a ten ohm standard. Since the room temperature varied less than $3^{\circ}C$ from the calibration temperature, no attempt was made to correct the resistance readings for variation in bridge temperature. After all calibration procedures were considered, the absolute accuracy of the temperature measurement is $\pm$ $0.03^{\circ}C$.

VI. EXPERIMENTAL RESULTS

A. MEASUREMENT OF THE RETARDATION

In the introduction, the possibility of doing three new types of measurements, progressive, pulsed progressive and time coincidence measurements was discussed. In the theory section, the retardation "v" was calculated as a function of the distance from the transducer and ratio of transducer radius to wavelength. Also, in the theory section, the effect of diffraction on sound velocity measurements was discussed. Before the discussion of sound velocity measurements, one check upon the correctness of the theory can be made by measuring the magnitude of the retardation "v" as a function of z. Sound beams from both the 1 mHz and 2 mHz transducers were investigated with a zeroth order schlieren optical system. From the photograph Fig. 4 (made up of a series of photographs) one can see that the near field radiation pattern is quite complicated. The relative retardation through the sound beam diameter (center of the picture) was measured by varying the transducer potential in such a manner that the retardation was held at a constant value. This was judged by eye or by a photomultiplier microphotometer located at the center of the schlieren image. Then the inverse of the transducer potential so measured is proportional to the retardation. These experimental measurements are plotted on graphs along with the exact expression in Figs. 14 and 15 for 2 mHz and 1 mHz respectively. Agreement is good in the two figures except near the transducer; however, the variation in the measured

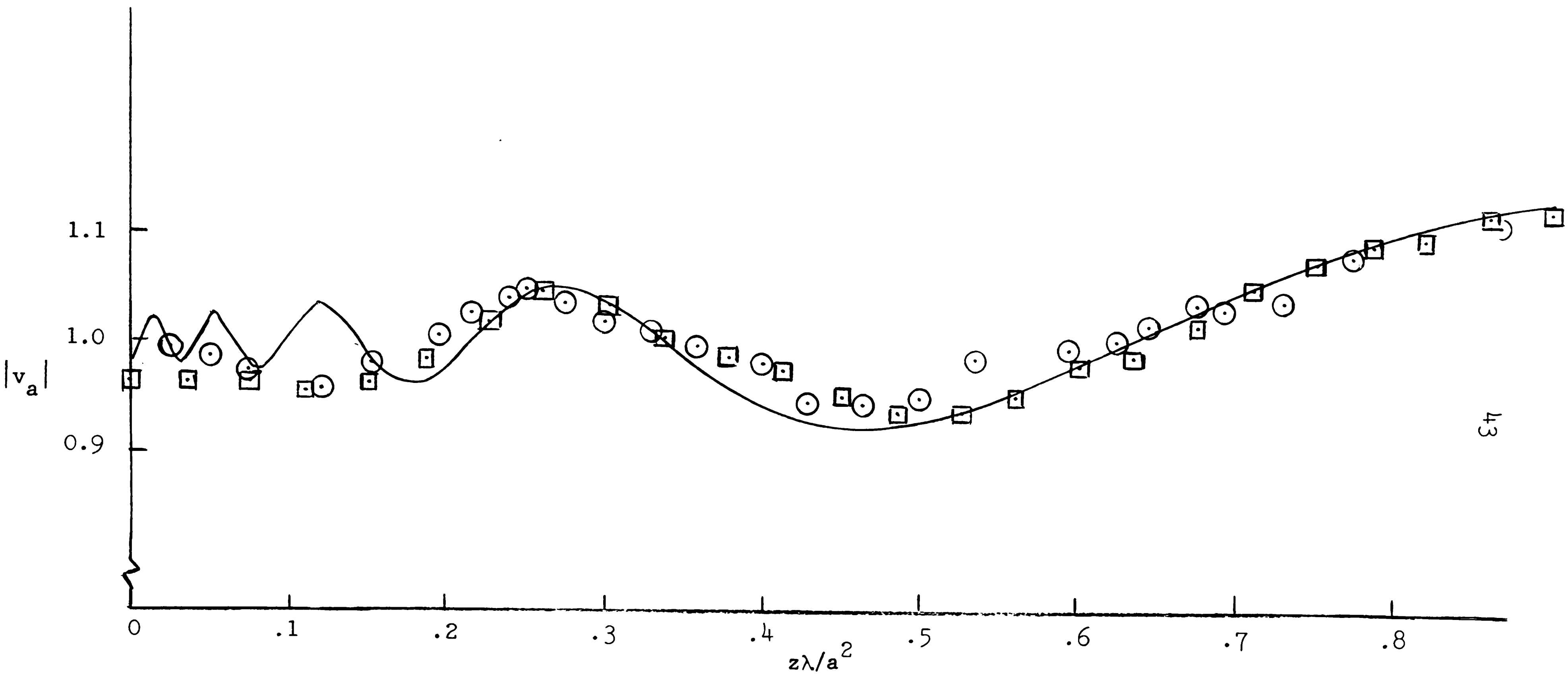

Figure 14. Measured Axial Retardation for 2 mHz, 22 mm dia., a 15λ data points

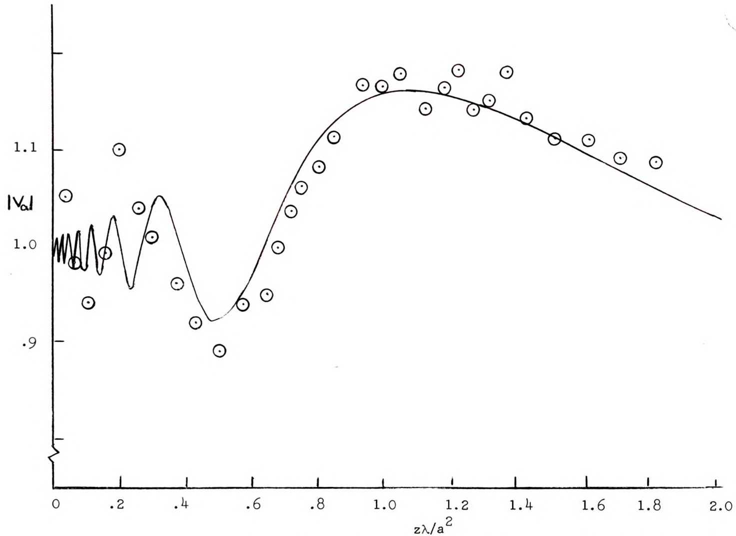

Figure 15. Measured Axial Retardation for a 1 mHz, 25.4 mm dia., transducer.

retardation for the 2 mHz transducer is less then theoretical curve. Note that the scales on the two graphs are not the same. For the calibration of transducers this agreement between the mathematical expression for the retardation and that obtained experimentally is of vital concern. Also, those making attenuation measurements using optical methods may benefit from this "diffraction correction".

B. SOUND VELOCITY MEASUREMENTS

As indicated in the preceding section, the magnitude of the calculated retardation and the experimental retardation agree except very near the transducer. From this encouraging agreement one would hope that the relative phase of this retardation would also agree with experiment. This relative phase variation represents a small systematic variation in the measured wavelength intervals. In order to ascertain this variation, the position of every third wavelength (as indicated by the closing of a Lissajous pattern) was measured for the 1 mHz transducer. Transducer positions were recorded over a distance of approximately 14 cm. which means that the dimensionless parameter $z\lambda/a^2$ varied from 0 to 1.4. These points may be fitted to a theoretical relative phase curve by estimating the plane wave phase velocity, calculating the plane wave phase and then subtracting the plane wave phase from the measured phase. This attempt is shown in Fig. 16.

There is quite a bit of scatter in the experimental points, however, the general trend is clearly evident. The sound velocity (extrapolated to 34.00°C) which was chosen to fit the curve was 1517.6 m/sec. The tail of the curve would fit better if this value was raised to 1517.7 m/sec. The scatter in the points is approximately .06 radians which would give an error in the velocity of $\pm$ .2 m/sec over the entire range.

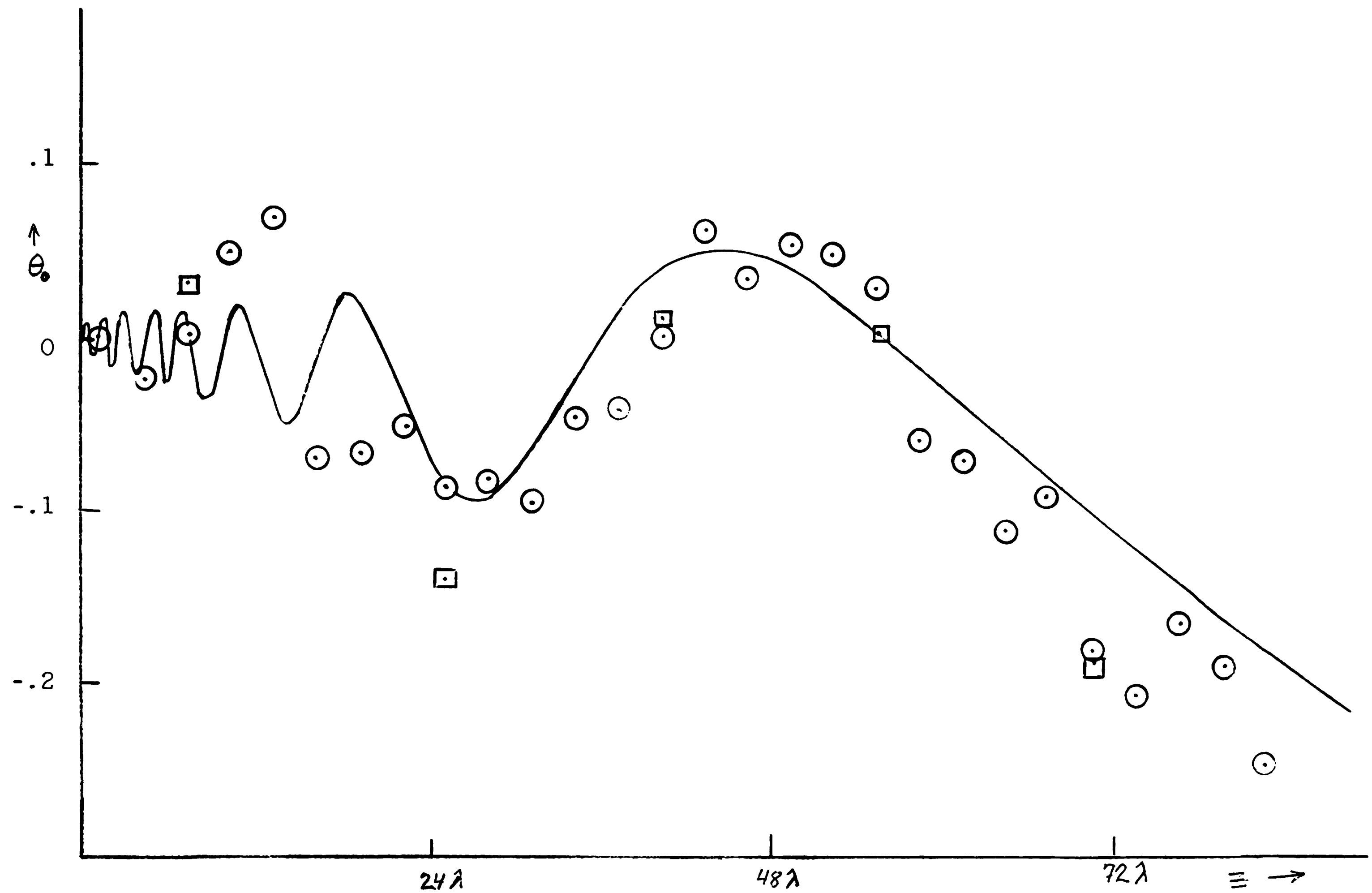

Figure 16. Measured Axial Relative Phase. [1mHz , diameter 25.4 mm.]
Theoretical curve (solid line) calculated from Eq. 13.

The sound velocity measurements using pulsed and continuous progressive wave techniques are shown in Table 2. Perhaps one of the most important results is shown in section 8a) in which a comparison was made between the continuous wave and pulsed continuous wave measurements. The two sets of data were obtained essentially simultaneously as the transducer was alternately connected to the output of the pulsed oscillator and then the transmitter. The two sets of data are in agreement within the precision of the measurements.

The first four measurements done with the Michelson interferometer were attempts to find variations in the wavelength near the transducer by measuring a few wavelengths at a time. The resulting errors are quite large because of the start - stop errors in the interferometer counting.

With the exception of the 6 mHz data all the measurements in Section B were corrected for diffraction errors by using the technique described in the chapter titled Theoretical Results. The diffraction corrections were, in all cases, smaller than those which would be applied if the geometrically equivalent experiment were performed using two similar transducers. As can be seen in Fig. 17, for diffraction corrections near the transducer the results of DelGrosso show much larger errors. Also, because this curve is nearly monotonic it is much more difficult to detect systematic errors caused by diffraction in a two transducer arrangement, when the frequency is low and not varied.

Table 2. Progressive Wave Measurements

A. Michelson Interferometer Length Measurements

Freq. (mHz)	Technique	$C_{34.00^o}$ (m/sec)
0.8	cw	1515.6 ± 2
0.8	cw	1517.0 ± 1
4.0	cw	1517.6 ± 2
1.0	cw	1518.7 ± 3 (individual λ's)
1.76	cw	1517.64 ± .25
5.28	cw	1517.76 ± .20
5.28	cw	1517.81 ± .20
	average of last 3	1517.73 ± .20

B. Gauge Block Length Measurement

a) 2.0	cw	1517.56 ± .20	comparison between pulsed and cw
2.0	pcw	1517.63 ± .20	
b) 1.0	cw	1517.70 ± .20	
2.0	cw	1517.66 ± .20	
2.0	cw	1517.62 ± .20	
2.0	cw	1517.72 ± .20	
2.0	pcw	1517.66 ± .15	
2.0	pcw	1517.62 ± .20	
6.0	cw	1517.63 ± .20	
6.0	pcw	1517.56 ± .20	
	average	1517.65 ± .20	

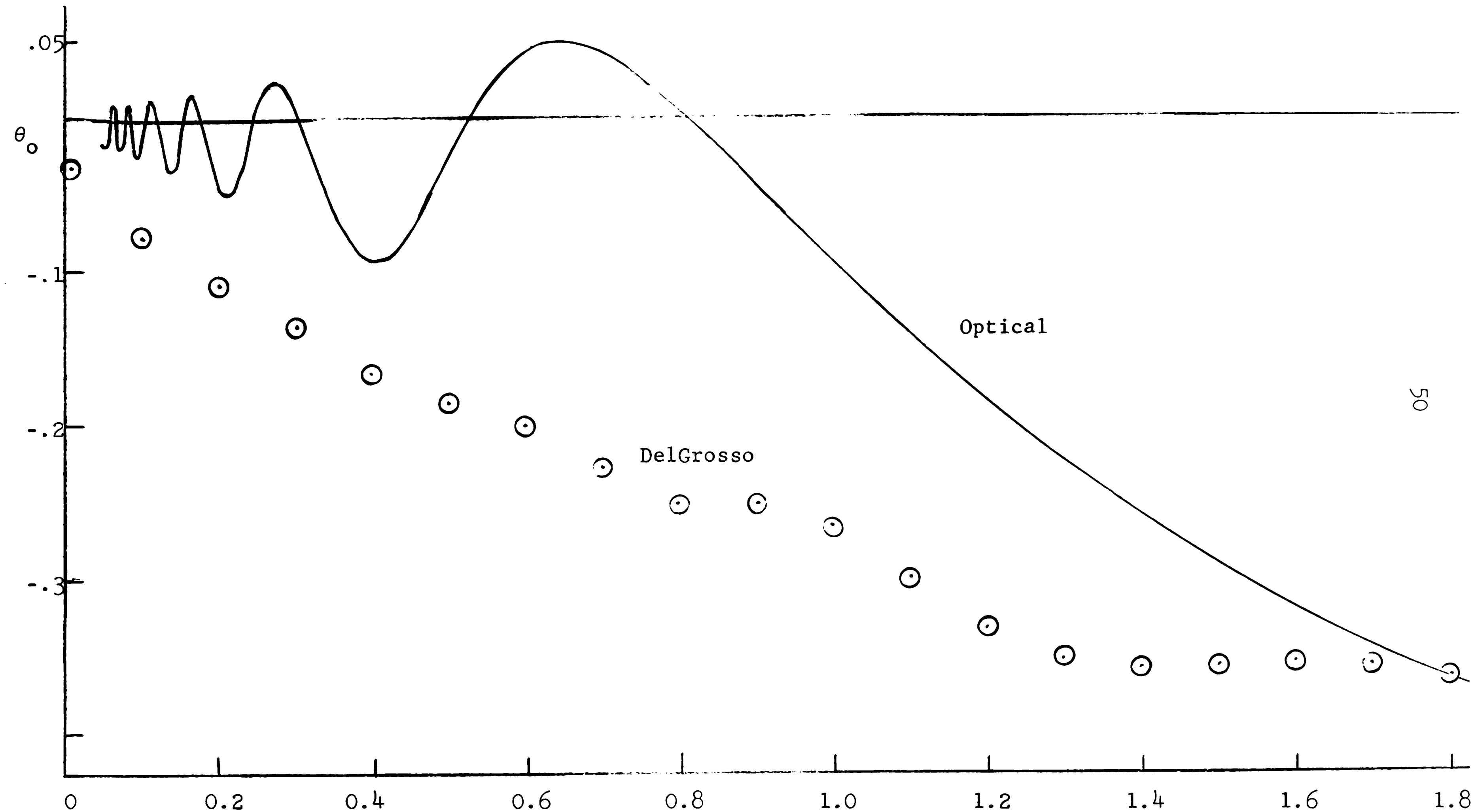

Figure 17. Relative Phase - Comparison of DelGrosso and Optical results ($a = 10\lambda$).

The pulsed time coincidence technique was used to make a velocity measurement at only one frequency because of the limitations imposed by the pulsing equipment. At high repetition rates, a pulse width of 1 μsec was the maximum allowable, and in order to have several cycles in the pulse envelope a transducer operating frequency of 6 mHz was chosen. The sound velocity adjusted to 34.00°C was 1517.53 m/sec $\pm$ .24. At 6 mHz, the maximum difference between the velocities obtained by continuous wave measurements (phase velocity) and pulse measurements (group velocity) for our configuration, is -0.10 m/sec (caused by geometrical "dispersion").

The standing wave measurements (see Table 3) demonstrate the same "dispersion" that was observed by Schreuer[13] and has recently been noted in interferometer measurements by Ilgunas[6] and others. The velocities made at 0.8 mHz and 1 mHz are considerably higher than the rest of the measurements made at higher frequencies. Neither the general diffraction correction suggested by Bass[20] nor the interferometer calculations by DelGrosso[9] predict such a large deviation at these frequencies and transducer configurations, Ilgunas has obtained similar large deviations in the acoustic interferometer. At higher frequencies, measured values fall about the value 1517.7 m/sec when the measurement cavity was long enough to permit a length measurement of adequate precision (about 70 to 90 mm.). One exception is the measurement at 7.2 mHz which is low.

Table 3. Standing Wave Measurements

A. Michelson Interferometer Length Measurement

f(mHz)	Cavity Length (mm)	$C_{34.00°}$(m/sec)
0.8	49	1518.50 ± 1.5
0.8	87	1518.86 ± 1.5
0.8	87	1519.14 ± .90
0.8	87	1518.28 ± .50
2.4	87	1518.10 ± .50
2.4	87	1517.67 ± .50
2.4	87	1517.82 ± .90
4.0	87	1517.77 ± .20
5.6	87	1517.60 ± .30
5.6	87	1517.68 ± .25
7.2	87	1517.44 ± .26

weighted average $C_{34.00°} = 1517.70 \pm .20$

1	47	1519.24 ± .20
1	87	1519.23 ± .40
1	23	1518.7 ± .60
2	74	1517.68 ± .20
2	21	1518.7 ± 1.0
6	84	1517.73 ± .18

weighted average $C_{34.00°} = 1517.70 \pm .20$

The grand weighted average of all the standing wave measurements is 1517.70 $\pm$ .25 (at 34.00°C) where the error limits now include the uncertainty in the absolute temperature measurement. There was good agreement between the values obtained with the two different measuring techniques (Johannasen gage blocks and Michelson interferometer) which would indicate that the systematic error inherent in the length measurements is quite small. DelGrosso's most recent measurements, when extrapolated to 34.00°C with Greenspan's data give a velocity of 1517.79 $\pm$ .02 m/sec. There is a difference of about .10 m/sec which is within the experimental error of the present experiments. The wavelength intervals for a given transducer, reflector and frequency were not constant over the length of the ultrasonic cavity. Near the reflector the intervals were longer which gave an apparent sound velocity higher than the average sound velocity by 0.5 to 6.0 m/sec. These differences were found to be approximately inversely proportional to the frequency. This strange behavior might explain some of the "random" fluctuations in Schreuer's measurements; he chose locations in the sound field where the visibility fringes were clear over 3-5 cm but didn't necessarily limit his measurements to those points far from the transducer. An explanation for this behavior might be sought in diffraction effects at the reflector.

For all the measurements described here, the magnitude of the errors are these: a) temperature $\pm$ .08 m/sec; b) sample impurity + .02 m/sec; and c) length $\pm$ .15 m/sec. Thus, a grand average sound

velocity is 1517.70 ± .25 m/sec. Extrapolated to 30°C this value becomes 1509.03 ± .25 m/sec. As can be seen, this value is closer to the work of Neubauer and Dragonette and that of Ilgunas, although, considering the magnitude of the uncertainty it is also near DelGrosso's current value.

This work has demonstrated that optical methods may be used to give sound velocity values in transparent media which are in agreement with other methods. Also, the errors caused by diffraction in the near field of the transducer are small and easily calculated, for the case of progressive waves. For the standing wave measurements, the appropriate corrections have not been calculated. For low frequencies the errors are very large and the corrections of Bass and DelGrosso are too small. Also, the corrections of Bass and DelGrosso are too small for the case of an acoustic interferometer operating at low frequencies. Until better calculations are completed (although the author has nothing to add to the careful and extensive calculations of DelGrosso) it seems that, for frequencies below 1 mHz and for small transducers the progressive wave optical methods together with a diffraction calculation which is accurately known might be the best way to measure sound velocities.

BIBLIOGRAPHY

1) A. B. Wood, E. H. Brown and C. Cochrane, Proc. Roy. Soc. 103, 284 (1923).

2) E. A. Eckhardt, Phys. Rev. 24, 452 (1924).

3) A. Kundt and O. Lehmann, Ann. de Pogg. 63, 1 (1874).

4) Hubbard and Loomis, Nature CXX, 189 (1927); Phil. Mag. 5, 1177 (1928).

5) V. A. DelGrosso et. al., N.R.L. Report 4439 (1954).

6) V. Ilgunas, O. Kubilyurere and A. Lapertas, Sov. Phys. Acoustics 10, 44 (1964).

7) V. A. DelGrosso, N.R.L. Report 6026 (1964).

8) V. A. DelGrosso, N.R.L. Report 6133 (1965).

9) V. A. DelGrosso, N.R.L. Report 6409 (1966).

10) Ch. Bachem and E. Hiedemann, Z. Physik 91, 418 (1934).

11) Ch. Bachem and E. Hiedemann, Z. Physik 91, 418 (1934).

12) Ch. Bachem, Z. Physik 101, 541 (1936).

13) E. Schreuer, Acousische Z. 4, 215 (1939).

14) N. Seifen, Z. Physik 108, 681 (1938).

15) M. Grabau, J. Acoust.Soc. Am. 5, 1 (1933).

16) E. Grossmann, Phys. Zeits. 35, 83 (1934).

17) E. Grossmann and E. Hiedemann, Z. Physik 95, 383 (1935).

18) M. Greenspan and C. E. Tschiegg, Bur. Standards J. Research, paper 2795, 59, 249 (1957).

19) V. A. DelGrosso, Paper at O.N.R. workshop, 21. June (1966).

20) H. J. McSkumin, J. Acoust.Soc. Am. 37, 325 (1965).

21) W. G. Neubauer and L. R. Dragonette, J. Acous. Soc. Am. 36, (1964).

22) R. Brooks, J. Acoust. Soc. Am. 32, 1422 (1960).

23) H. J. McSkimin, J. Acoust. Soc. Am. 29, 1185 (1957).

24) V. F. Nozdrev, The Use of Ultrasonics in Molecular Physics. Pergamon Press (1965), useful for the Russian references.

25) L. Bergmann, Der Ultraschall, Springer Verlag, (1949).

26) E. Hiedemann, Ch. Bachem and H. R. Asbach, Z. Physik 87, 734 (1934).

27) O. Nomoto, Phys. Math. Soc. Jap. Proc. 18, 402 (1936); 19, 337 (1937).

28) Lord Rayleigh, The Theory of Sound, Dover Publications, N.Y. (1945).

29) H. Bateman, Mathematical Analysis of Electrical and Optical Wave Motion, Cambridge Univ. Press (1915).

30) V. King, Canad. J. Res. 11, 135 (1934).

31) P. R. Pisharoty, Proc. Ind. Acad. Sci. 4, 27 (1936).

32) A. J. Crandall, M. S. Thesis, Michigan State Univ. (1964).

33) J. Meizner and U. Fritze, Z. angew. Physik 12, 36 (1949).

34) H. Seki, A. Granato and R. Turell, J. Acoust. Soc. Am. 28, 230 (1956).

35) A. O. Williams, Jr., J. Acoust. Soc. Am. 19, 150 (1947).

36) E. A. Hiedemann and S. K. Osterhammel, Z. Physik 107, 273 (1937).

37) E. A. Hiedemann and S. K. Osterhammel, Proc. Ind. Acad. Sci. (A) 8, 275 (1938).

38) S. K. Osterhammel, Akust. Z. 6, 73 (1941).